

High quality single-crystal germanium-on-insulator on bulk Si substrates based on multistep lateral over-growth with hydrogen annealing

Hyun-Yong Yu, Szu-lin Cheng, Jin-Hong Park, Ali K. Okyay, M. Cengiz Onbaşlı, Burcu Ercan, Yoshio Nishi, and Krishna C. Saraswat

Citation: *Appl. Phys. Lett.* **97**, 063503 (2010);

View online: <https://doi.org/10.1063/1.3478242>

View Table of Contents: <http://aip.scitation.org/toc/apl/97/6>

Published by the [American Institute of Physics](#)

Articles you may be interested in

[Defects reduction of Ge epitaxial film in a germanium-on-insulator wafer by annealing in oxygen ambient](#)
APL Materials **3**, 016102 (2015); 10.1063/1.4905487

[Reduced pressure–chemical vapor deposition of Ge thick layers on Si\(001\) for 1.3–1.55- \$\mu\text{m}\$ photodetection](#)
Journal of Applied Physics **95**, 5905 (2004); 10.1063/1.1699524

[Effects of hydrogen annealing on heteroepitaxial-Ge layers on Si: Surface roughness and electrical quality](#)
Applied Physics Letters **85**, 2815 (2004); 10.1063/1.1802381

[High quality Ge on Si by epitaxial necking](#)
Applied Physics Letters **76**, 3700 (2000); 10.1063/1.126754

[High-quality Ge epilayers on Si with low threading-dislocation densities](#)
Applied Physics Letters **75**, 2909 (1999); 10.1063/1.125187

[High-quality single-crystal Ge on insulator by liquid-phase epitaxy on Si substrates](#)
Applied Physics Letters **84**, 2563 (2004); 10.1063/1.1691175



The advertisement features the Lake Shore CRYOTRONICS logo on the left, which includes a stylized blue square icon. In the center, there is a photograph of the 8600 Series VSM (Vibrating Sample Magnetometer) instrument, showing a computer monitor displaying data, a control panel, and the main measurement chamber with a sample mounted on a rotating stage. To the right of the image, the text reads "8600 Series VSM" in large orange letters, followed by "For fast, highly sensitive measurement performance" in white. At the bottom right, there is a "LEARN MORE" button with a right-pointing arrow.

High quality single-crystal germanium-on-insulator on bulk Si substrates based on multistep lateral over-growth with hydrogen annealing

Hyun-Yong Yu,^{1,a)} Szu-lin Cheng,¹ Jin-Hong Park,^{1,2} Ali K. Okyay,^{3,4} M. Cengiz Onbaşlı,³ Burcu Ercan,² Yoshio Nishi,¹ and Krishna C. Saraswat¹

¹Department of Electrical Engineering, Stanford University, Stanford, California 94305, USA

²Department of Electronics and Radio Engineering, College of Electronics and Information, Kyung Hee University, Yongin-si/Gyeonggi-do 446-701, Republic of Korea

³Department of Electrical and Electronics Engineering, Bilkent University, Ankara 06800, Turkey

⁴UNAM, Institute of Materials Science and Nanotechnology, Bilkent University, Ankara 06800, Turkey

(Received 21 June 2010; accepted 21 July 2010; published online 9 August 2010)

Germanium-on-insulator (GOI) is desired for high performance metal-oxide-semiconductor transistors and monolithically integrated optoelectronics. We demonstrate a promising approach to achieve single-crystal defect-free GOI by using lateral over-growth through SiO₂ window. The dislocations due to the lattice mismatch are effectively terminated and reduced in SiO₂ trench by selective area heteroepitaxy combined with hydrogen annealing. Low defect density of $4 \times 10^6 \text{ cm}^{-2}$ and low surface roughness of 0.7 nm (root-mean-square) on GOI are confirmed by plan-view transmission electron microscopy and atomic force microscopy analysis. In addition, the excellent metal-semiconductor-metal diode electrical characteristics fabricated on this GOI confirm Ge crystal quality. The selectively grown GOI structure can provide the monolithic integration of SiGe based devices on a Si very large scale integration (VLSI) platform. © 2010 American Institute of Physics.

[doi:10.1063/1.3478242]

Germanium has been considered as a promising material for high performance complementary metal-oxide-semiconductor (CMOS) transistors and optoelectronic applications as it offers much higher and symmetric carrier mobility¹⁻³ and smaller optical band gap ideal for 1.3–1.5 μm wavelength commonly used in telecommunication.⁴ Germanium-on-insulator (GOI) can specially provide high performance MOS field-effect transistors by high-speed operation as well as low parasitic capacitance and immunity for short channel effects. Low-leakage junction current by thin-body GOI is also another benefit for channel materials with smaller band gap.^{5,6} Even more research efforts are directed toward the realization of on-chip optical signaling using Ge-based devices. There has been a surge in interest in SiGe based optoelectronics such as near IR detectors,⁷⁻⁹ Ge-based integrated optical modulators,^{10,11} and so on. The marriage of microelectronics to high performance photonics requires precise control and process compatibility. It is hence crucial to be able to grow high quality SiGe layers selectively on Si. For GOI structures, currently, many techniques such as oxidation-induced Ge condensation,¹² laser annealing,^{13,14} solid-phase crystallization,^{15,16} metal-induced lateral crystallization,¹⁷ bonding,¹⁸ and lateral epitaxial growth¹⁹ have been introduced. However, these techniques to obtain GOI structures can be very complicated and have difficulty in achieving high-quality Ge films. In addition, the monolithic integration with Si based CMOS technology seems to be much more difficult. In other material, such as GaN, lateral overgrowth technique has been demonstrated to effectively reduce dislocation densities on GaN films and was used to fabricate very high performance light emitting diodes and laser diodes.²⁰⁻²²

In this paper, we demonstrate the lateral overgrowth of germanium on a SiO₂ layer with multistep lateral overgrowth with hydrogen annealing (MLHA) technique. This MLHA technique yields Ge layers with very low dislocation density and surface roughness as confirmed by transmission electron microscope (TEM) analysis, and atomic force microscope (AFM) surface morphology studies. In addition, metal-semiconductor-metal (MSM) diode electrical characteristics are shown to confirm Ge crystal quality on SiO₂.

A SiO₂ layer was thermally grown on p-type (100) Si substrate at 1100 °C that finally became the insulator layer of the GOI structure. The SiO₂ film was then patterned by dry-etching followed by wet-etching. These etched vias became the growth windows for selective Ge epitaxy. The starting surface is very critical in epitaxy for single-crystal growth; therefore, the samples were etched in 50:1 (H₂O:HF) for 30 s and immediately loaded into an Applied Materials Centura epitaxial reactor. A hydrogen bake at 1000 °C was carried out to ensure that no native oxide remained on the Si surface between SiO₂ walls. In order to increase the resulting films quality, a very thin Si epilayer was first grown for 90 s at 700 °C with dichlorosilane as the reaction species.

Ge growth on Si is surface reaction limited below 450 °C and is mass transport limited above.²³ Therefore, low growth temperatures and pressures provide better selectivity between Si and SiO₂. The reaction temperature was found to influence the growth rates of different crystal directions, as reported elsewhere.²⁴ At 400 °C, ⟨100⟩ normal direction was dominant at 30 nm/min compared to 3 nm/min in ⟨113⟩ direction. This resulted in facet formation with {113} surfaces. At elevated temperatures such as 600 °C, growth rates for ⟨100⟩ and ⟨113⟩ directions were 60 nm/min and 12 nm/min, respectively. Therefore, a careful design of the growth con-

^{a)}Electronic mail: yuhykr@stanford.edu.

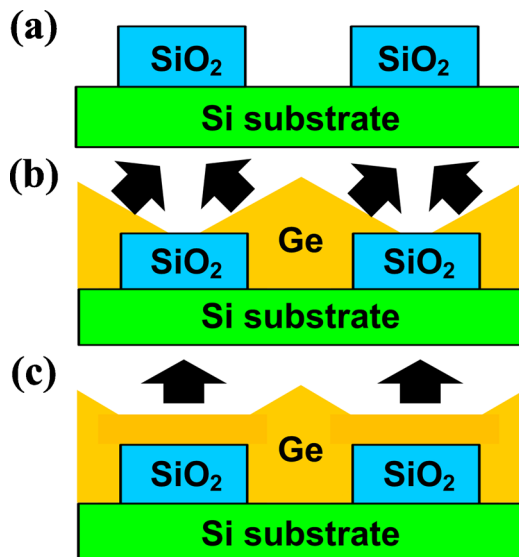


FIG. 1. (Color online) Illustration (a) of selective Ge growth at 400 °C on Si through openings in the SiO₂ film. (b) Illustration of the growth mechanism at 400 °C before the films coalesce, (c) growth at 600 °C after coalescence.

ditions and a trade off between nucleation/selectivity and growth rate is required to achieve high quality GOI virtual substrates. Figure 1 shows the schematic of the lateral overgrowth Ge process. As shown Fig. 1(a), an initial low-temperature growth is performed for higher Si–SiO₂ selectivity and reduced surface roughness. Once Ge layer becomes pyramidlike shape in the SiO₂ trench, <311> direction growth becomes dominant before coalescences in Fig. 1(b). After the coalescence happens, <100> direction growth starts at the valley where two Ge growth fronts meet at specific condition. As shown in Fig. 1(c), due to a higher growth rate of <100> direction compared to that of <311> direction, the valley is quickly filled up and <100> growth is dominant.

The initial Ge layer was grown at 400 °C with a partial pressure of 8 Pa. Temperature in the chamber was raised to 825 °C and the sample was annealed for 30 min in H₂ ambient. This step is crucial to allow for surface reconstruction, reduce dislocation density and surface roughness.^{23,25} An

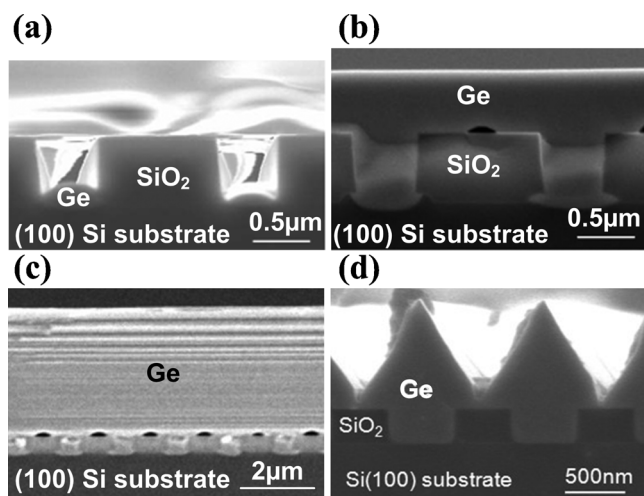


FIG. 2. Cross-sectional SEM images of the film after (a) growth at 400 °C, (b) growth at 400 °C followed by 15 min at 600 °C, (c) growth at 400 °C followed by 35 min at 600 °C, and (d) growth at 400 °C for 1 h.

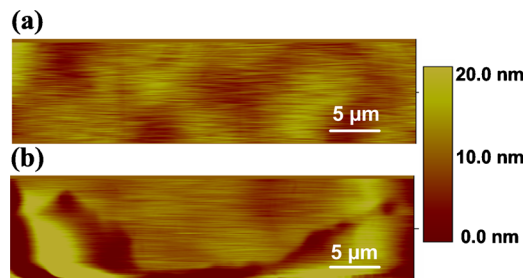


FIG. 3. (Color online) AFM scan images of 40 × 10 μm² of the resulting thick film after low-temperature (400 °C) and high-temperature (600 °C) growth (a) with and (b) without intermediate H₂ anneal steps.

scanning electron microscopy (SEM) image of the sample after this step is shown in Fig. 2(a). After the coalescence, an additional growth step was performed at 600 °C for 15 min followed by H₂ annealing at 825 °C, where the valley was filled up due to fast <100> direction growth. However, as shown in Fig. 2(d), <100> direction growth does not start at the valley after the coalescence of Ge films at 400 °C additional growth step. Figure 2(b) shows the resulting lateral over-lateral growth with the 400 °C and 600 °C growth temperature combination. The overall Ge layer thickness can be increased by longer growth at 600 °C as demonstrated in Fig. 2(c) for a growth time of 35 min.

Large surface roughness and dislocation density are observed on as-grown samples as a result of the 4.2% lattice mismatch between Si and Ge. The surface roughness reduction by annealing in hydrogen ambient at 825 °C is attributed to hydrogen-mediated Ge diffusion and the reconstruction of the surface.²³ Figure 3 shows 40 × 10 μm² AFM scan images for two lateral overgrowth Ge films grown without hydrogen annealing and with MLHA. The surface of the sample with no annealing was significantly smoothed with MLHA. A very low rms surface roughness of 0.7 nm was achieved in MLHA GOI samples down from 3.5 nm for unannealed GOI films.

GOI film quality was investigated by TEM analysis. TEM images in Fig. 4 show very high quality Ge layers obtained on SiO₂. Ge film grows selectively through a 500 nm wide window in the SiO₂ layer. Defects were found only in the first 60 nm thick region from the Ge and Si interface. Previous efforts to obtain high quality epilayers on

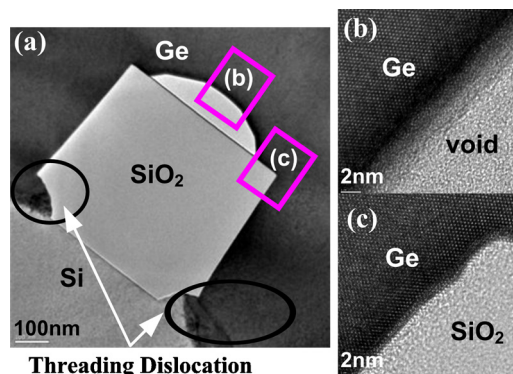


FIG. 4. (Color online) (a) Cross sectional TEM (XTEM) image of grown Ge film and the SiO₂ mesa block. Defects and dislocations are in close vicinity of the Ge–Si interface while the rest of the film has very low defect density. [(b) and (c)] High resolution XTEM images of the Ge film on top of the SiO₂ mesa and the void, showing defect free GOI layers.

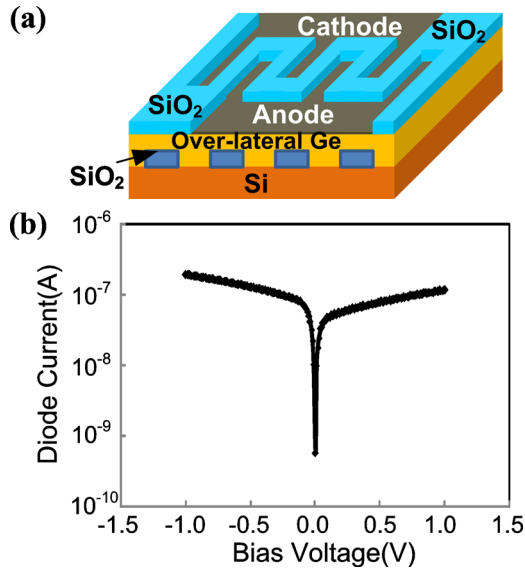


FIG. 5. (Color online) (a) Cross-section of MSM diode fabricated on over-lateral grown Ge layer. (b) Current vs voltage characteristics of metal-semiconductor (Ti-Ge) Schottky diode on over-lateral grown GOI, both forward and reverse bias regions.

Si required a 500 nm or thicker buffer layers to confine the defects and dislocations.^{10,26} The hydrogen annealing technique reported in this work increases the surface mobility of Ge atoms leading dislocations to glide to Ge/SiO₂. In other word, the SiO₂ sidewalls provide sinks for the dislocations. Once the Ge film thickness exceeds the height of the SiO₂ trench, the lateral overgrowth of the film results in extremely single-crystal GOI layer. Owing to MLHA, the lateral overgrown Ge layer shows very low defect density, having a threading dislocation density count of $\sim 4 \times 10^6 \text{ cm}^{-2}$ based on the plan view TEM analysis. Figures 4(b) and 4(c) also show no visible defect where the growth fronts join. This is attributed to dislocation trapping within SiO₂ trenches.

In order to confirm the high crystal quality of Ge layer over-laterally grown on SiO₂ electrically, we fabricated simple MSM diode with interdigitated electrode width (5 μm) and spacing (5 μm) on the top of the over-lateral grown Ge layer. A 200 nm thick low-temperature chemical-vapor-deposited oxide layer was deposited at 400 °C for the purpose of surface passivation and isolation. This oxide layer was lithographically patterned and HF-etched, followed by metal electrode e-beam evaporation and photoresist lift-off process. Figure 5(a) illustrates a schematic diagram of the final structure. 15 nm thick Ti was used for controlling work function as well as achieving good adhesion, and then it was topped with 35 nm thick Au. Figure 5(b) presents the electrical current-voltage (I-V) characteristic of MSM (Ti-Ge-Ti) diode. Therefore, high quality Ge layer introduces low leakage current.²⁷ Back-to-back Schottky diode behavior and low leakage current of $1.18 \times 10^{-7} \text{ A}$ at 1 V as shown in Fig. 5 confirms the excellent Ge crystal quality of over-lateral grown GOI substrate.

In conclusion, we have demonstrated very high quality and defect free GOI with MLHA. The multistep 400/600 °C

growth mechanism achieves single-crystal GOI. The MLHA. This MLHA technique yields Ge layers with very low dislocation density and surface roughness. Such an approach promises the integration of SiGe based devices on a Si very large scale integration (VLSI) platform.

This work was performed at the Stanford Nanofabrication Facility (SNF) and was supported by MARCO Interconnect Focus Centers and the Stanford University INMP. The authors are grateful to Ted Kamins for helpful discussion.

- ¹C. O. Chui, H. Kim, D. Chi, B. B. Triplett, P. C. McIntyre, and K. C. Saraswat, Tech. Dig. - Int. Electron Devices Meet. **2002**, 441.
- ²C. H. Lee, T. Nishimura, N. Saito, K. Nagashio, K. Kita, and A. Toriumi, Tech. Dig. - Int. Electron Devices Meet. **2009**, 457.
- ³H.-Y. Yu, M. Ishibashi, J.-H. Park, M. Kobayashi, and K. C. Saraswat, *IEEE Electron Device Lett.* **30**, 675 (2009).
- ⁴K. Saraswat, D. Kim, T. Krishnamohan, D. Kuzum, A. Okyay, A. Pethé, and H.-Y. Yu, *ECS Trans.* **16**(10), 3 (2008).
- ⁵S.-I. Takagi, Dig. Tech. Pap. - Symp. VLSI Technol. **2003**, 115.
- ⁶T. Maeda, K. Ikeda, S. Nakaharai, T. Tezuka, N. Sugiyama, Y. Moriyama, and S. Takagi, *Thin Solid Films* **508**, 346 (2006).
- ⁷M. Oehme, J. Werner, E. Kasper, M. Jutzi, and M. Berroth, *Appl. Phys. Lett.* **89**, 071117 (2006).
- ⁸D. Ahn, C. Hong, J. Liu, W. Giziewicz, M. Beals, and L. C. Kimerling, *Opt. Express* **15**, 3916 (2007).
- ⁹H.-Y. Yu, S. Ren, W. S. Jung, A. K. Okyay, D. A. B. Miller, and K. C. Saraswat, *IEEE Electron Device Lett.* **30**, 1161 (2009).
- ¹⁰Y. H. Kuo, Y. Lee, Y. Ge, S. Ren, J. E. Roth, T. I. Kamins, D. A. B. Miller, and J. S. Harris, *Nature (London)* **437**, 1334 (2005).
- ¹¹O. Fidaner, A. K. Okyay, J. E. Roth, R. K. Schaevitz, Y. H. Kuo, K. C. Saraswat, J. S. Harris, and D. A. B. Miller, *IEEE Photonics Technol. Lett.* **19**, 1631 (2007).
- ¹²S. Nakaharai, T. Tezuka, N. Sugiyama, Y. Moriyama, and S. Takagi, *Appl. Phys. Lett.* **83**, 3516 (2003).
- ¹³H. Watakabe, T. Sameshima, H. Kanno, T. Sadoh, and M. Miyao, *J. Appl. Phys.* **95**, 6457 (2004).
- ¹⁴W. Yeh, H. Chen, H. Huang, C. Hsiao, and J. Jeng, *Appl. Phys. Lett.* **93**, 094103 (2008).
- ¹⁵T. Tsunoda, A. Kenjo, T. Sadoh, and M. Miyao, *Appl. Surf. Sci.* **224**, 231 (2004).
- ¹⁶C. Y. Tsao, J. W. Weber, P. Campbell, P. I. Widenborg, D. Song, and M. A. Green, *Appl. Surf. Sci.* **255**, 7028 (2009).
- ¹⁷J.-H. Park, P. Kapur, H. Peng, and K. C. Saraswat, *Appl. Phys. Lett.* **91**, 143107 (2007).
- ¹⁸M. N. Kamalasanan, S. Chandra, P. C. Joshi, and A. Mansingh, *Appl. Phys. Lett.* **59**, 3547 (1991).
- ¹⁹V. D. Cammilleri, V. Yam, F. Fossard, C. Renard, D. Bouchier, P. F. Fazzini, L. Ortolani, F. Houdellier, and M. Hytch, *Appl. Phys. Lett.* **93**, 043110 (2008).
- ²⁰H. Marchand, X. Wu, J. Ibbetson, P. Fini, P. Kozodoy, S. Keller, J. Speck, S. DenBaars, and U. Mashra, *Appl. Phys. Lett.* **73**, 747 (1998).
- ²¹A. Usui, H. Sunakawa, A. Sakai, and A. Yamaguchi, *Jpn. J. Appl. Phys., Part 2* **36**, L899 (1997).
- ²²S. Nakamura, M. Senoh, S. Nagahama, N. Iwasa, T. Yamada, T. Matsushita, H. Kiyoku, Y. Sugimoto, T. Kozaki, H. Umemoto, M. Sano, and K. Chocho, *Jpn. J. Appl. Phys., Part 2* **36**, L1568 (1997).
- ²³A. Nayfeh, C. O. Chui, and K. C. Saraswat, *Appl. Phys. Lett.* **85**, 2815 (2004).
- ²⁴J.-S. Park, J. Bai, M. Curtin, B. Adekore, M. Carroll, and A. Lochtefeld, *Appl. Phys. Lett.* **90**, 052113 (2007).
- ²⁵S. Kobayashi, M. Cheng, A. Kohlase, T. Sato, J. Murota, and N. Mikoshiba, *J. Cryst. Growth* **99**, 259 (1990).
- ²⁶H. Luan, D. Lim, K. Lee, K. Chen, J. Sandland, K. Wada, and L. Kimerling, *Appl. Phys. Lett.* **75**, 2909 (1999).
- ²⁷A. K. Okyay, A. M. Nayfeh, T. Yonehara, A. Marshall, P. C. McIntyre, and K. C. Saraswat, *Opt. Lett.* **31**, 2565 (2006).